Arnold Schwarzenegger
Governor

SCALE SELECTIVE BIAS CORRECTION IN A DOWNSCALING OF GLOBAL ANALYSIS USING A REGIONAL MODEL

PIER PROJECT REPORT

Prepared For:
California Energy Commission
Public Interest Energy Research Program

Prepared By:
Scripps Institution of Oceanography,
University of California, San Diego

August 2005
CEC-500-2005-130

California Climate Change Center
Report Series Number 2005-20

Prepared By:
Scripps Institution of Oceanography
University of California, San Diego
Hideki Kanamaru
Masao Kanamitsu
La Jolla, California 92093-0224
Contract No. 500-02-004
Work Authorization No. MR-004

Prepared For:
California Energy Commission
Public Interest Energy Research (PIER) Program

Guido Franco,
Contract Manager

Kelly Birkinshaw,
Program Area Team Lead
Energy-Related Environmental Research

Martha Krebs, Ph.D.
Deputy Director
ENERGY RESEARCH AND DEVELOPMENT DIVISION

B. B. Blevins
Executive Director

Acknowledgements

The authors would like to thank California Energy Commission for the support of this research.

Please cite this report as follows:

Kanamaru, H., and M. Kanamitsu. 2005. *Scale Selective Bias Correction in a Downscaling of Global Analysis Using a Regional Model.* California Energy Commission, PIER Energy-Related Environmental Research. CEC-500-2005-130.

Preface

The Public Interest Energy Research (PIER) Program supports public interest energy research and development that will help improve the quality of life in California by bringing environmentally safe, affordable, and reliable energy services and products to the marketplace.

The PIER Program, managed by the California Energy Commission (Energy Commission), annually awards up to $62 million to conduct the most promising public interest energy research by partnering with Research, Development, and Demonstration (RD&D) organizations, including individuals, businesses, utilities, and public or private research institutions.

PIER funding efforts are focused on the following RD&D program areas:

- Buildings End-Use Energy Efficiency
- Energy-Related Environmental Research
- Energy Systems Integration
- Environmentally Preferred Advanced Generation
- Industrial/Agricultural/Water End-Use Energy Efficiency
- Renewable Energy Technologies

The California Climate Change Center (CCCC) is sponsored by the PIER program and coordinated by its Energy-Related Environmental Research area. The Center is managed by the California Energy Commission, Scripps Institution of Oceanography at the University of California at San Diego, and the University of California at Berkeley. The Scripps Institution of Oceanography conducts and administers research on climate change detection, analysis, and modeling; and the University of California at Berkeley conducts and administers research on economic analyses and policy issues. The Center also supports the Global Climate Change Grant Program, which offers competitive solicitations for climate research.

The California Climate Change Center Report Series details ongoing Center-sponsored research. As interim project results, these reports receive minimal editing, and the information contained in these reports may change; authors should be contacted for the most recent project results. By providing ready access to this timely research, the Center seeks to inform the public and expand dissemination of climate change information; thereby leveraging collaborative efforts and increasing the benefits of this research to California's citizens, environment, and economy.

The work described in this report was conducted under the Preliminary Climatic Data Collection, Analyses, and Modeling contract, contract number 500-02-004, work authorization MR-004, by the Scripps Institution of Oceanography.

For more information on the PIER Program, please visit the Energy Commission's website www.energy.ca.gov/pier/ or contract the Energy Commission at (916) 654-4628.

Table of Contents

Abstract

Systematic large-scale errors are often found within the regional domain in the regional dynamical downscaling procedure. This report proposes a method to suppress such error, using a combination of spectral tendency damping and area-average correction technique. The technique reduces the tendency of zonal and meridional wind components for the physical scale greater than a specified scale. In addition, the area mean perturbations of temperature and humidity are forced to zero, and the domain-averaged natural logarithm of surface pressure perturbation is set to the natural logarithm of the pressure difference of the mean surface elevation between the regional fine-scale field and the base coarse field. Each of these three components of the technique is necessary for the model to reduce large-scale errors in the regional domain effectively. With this method, the regional model is able to generate consistent analyses regardless of domain size. The downscaled field of precipitation compares better with observations. The lateral boundary relaxation is still an essential part of the regional model, but the proposed scheme allows larger e-folding time. The use of a similar scheme is recommended for any regional model in the application of dynamical downscaling to climate studies.

1.0 Introduction

Regional climate models are often used to dynamically produce high-resolution analysis of atmosphere and land that global data assimilation system can resolve only at coarse resolution. When the dynamical downscaling technique is used with reanalyses such as those from the National Centers for Environmental Prediction (NCEP) and the European Centre for Medium-Range Weather Forecasts (ECMWF), all the regional details are simulated by the regional model without an input of direct regional-scale observations. What drives the regional model is only the global reanalyses on coarse grids. Therefore, dynamical downscaling can be considered as a "poor person's data assimilation technique" (von Storch 2000) or a "regional data assimilation without regional observation."

Downscaling techniques are supposed to retain all the large-scale information that has been resolved well in the global reanalysis data assimilation and add smaller-scale information that the coarse-resolution global data assimilation model could not generate. Regional models, however, have to deal with the problem of lateral boundary conditions, which is mathematically ill posed. The inconsistencies between the model solution and the driving coarse model field along the boundaries produce undesirable noise, and often, instabilities. The lateral boundary relaxation method of Davies (1976) is usually used to alleviate such errors in a buffer zone that covers several grid points along the model boundary.

Systematic large-scale errors could also develop within the regional domain, due to model error. A large-scale solution on the scale of 5–6 grids of the driving global analysis should be trusted and the regional model is not meant to modify such large-scale fields when producing regional solutions. In reality, anomalous long waves could be found within the regional domain. Such waves reflect and interfere with shorter waves, distorting the circulation on regional scale. The change in domain-averaged temperature and moisture will impact the physical processes through changes in moisture availability and static stability. Most regional models predict full field within the regional model domain without any knowledge of large-scale features resolved by the driving global analysis, except in the buffer zone near the lateral boundaries through Davies-type relaxation . The interior of the domain away from the lateral boundaries is not directly driven by the state of large-scale climate in Davies-type relaxation, but the information at the boundary eventually propagates into the domain and provides the large-scale information inside the regional domain.

This notion of using global analysis in the inner domain has led to the "perturbation filter" method first proposed by Hoyer (1987), and used in more practical applications by Juang and Kanamitsu (1994) in the Regional Spectral Model (RSM) originally developed at NCEP. Global models and regional models have different spectral ranges, but they share the same physical scale (small scale for the global model, but large scale for the regional model). Hoyer (1987) and Juang and Kanamitsu (1994) proposed decomposing a full forecast model field within the regional domain into two components: base field and regional perturbation field. The base field is obtained from the global coarse grid over the entire regional model domain. The regional perturbation field is defined as a difference between the total field and the base field, and it is decomposed into sine and cosine series. This spectral representation provides a way to filter out those waves longer than the regional domain. Thus large-scale waves longer than the regional domain cannot be disturbed during the entire period of integration.

Most other regional models, however, do not use the perturbation method. They predict full regional fields in the regional domain. Waldron et al. (1996) suggested a spectral nudging technique that allows incorporation of large internal scales from the outer model into the regional domain for use in "full field" models. A nudging term is added to the tendencies of the variables such as zonal and meridional wind components in their grid point model. The nudging term is the summation of the difference between the spectrally expanded base field and the model field, multiplied by the nudging coefficients over selected wavenumbers. Von Storch et al. (2000) used the technique to nudge the long waves in the regional domain to those of the driving fields in a climate simulation study. The nudging coefficients varied with height: larger nudging coefficients higher in the atmosphere where confidence in the reanalysis is higher, smaller coefficients near the surface, and 0 in the boundary layer. The nudging term relaxes the selected long wave part of the spectrum to the corresponding waves from the driving fields.

In the RSM, any scales longer than the regional domain cannot be modified during the course of integration because only the perturbation from the underlying global field is predicted in the regional model. Although the global model field is used in the entire domain, it is only applied to reduce the error due to the Fourier transform of the regional scale field, and there is no explicit forcing towards global model field in the interior of the regional domain. Therefore, RSM is also susceptible to the large-scale error issues that Waldron et al. (1996) and von Storch et al. (2000) addressed.

This paper proposes a scheme called *Scale Selective Bias Correction* (SSBC), which is similar in function to those of von Storch et al. (2000) and Miguez-Macho et al. (2004), which both involve the application of spectral nudging technique. However, this new scheme is developed to work in the RSM.

It is noted that the regional dynamical "downscaling" should be clearly distinguished from regional "forecast," because the objectives of the two are very different. The objective of the former is to obtain regional detail, knowing the large-scale field from coarse-resolution analyses with sufficient accuracy; while that of the latter is to produce a good forecast in the regional domain with some reliance (although not entire reliance) on large-scale fields produced by global model forecast. In a regional "forecast," a regional model may be used to improve the large-scale field in the regional domain—particularly when the regional domain is large, because the large-scale field of global model forecast may contain errors. In regional "downscaling," on the other hand, the regional model should not modify the large-scale field in the regional domain because the large-scale field from the coarse-resolution base field is considered accurate.

Application of dynamical downscaling to global warming simulation is a little trickier, because global simulation contains significant errors, and regional model may not be able to rely entirely on the lateral forcing. However, it is also difficult to expect the regional model to improve the accuracy of the large-scale portion of the global warming simulations within the regional domain, because the one-way nesting prohibits the mutual interactions between global and regional scales. Note that a two-way nesting model cannot be used for "downscaling," since there is no way to force "analysis" or "forecast" from other models through lateral boundary conditions. It is emphasized that this paper specifically discusses the dynamical downscaling of the global analysis, where large-scale analysis is considered to be accurate.

The outline of this paper is as follows: Section 2.1 introduces the SSBC procedure. The property of the procedure is demonstrated and compared to von Storch's spectral nudging (von Storch et al. 2000) in Section 2.2. Section 2.3 shows that the SSBC method works to reduce the dependency of regional solution on the domain size. The choice of damping coefficient is discussed in Section 2.4. Section 2.5 discusses the relation between lateral relaxation and the SSBC method. Section 2.6 shows that the reduction of large-scale errors actually improves the downscaled field of precipitation verified against observations. Section 2.7 presents the changes in surface flux fields, to highlight the effect of the SSBC on physical processes in the model. Section 3 presents conclusions.

2.0 Experiments

The Regional Spectral Model (RSM) was originally developed at the National Metrological Center (NMC, formerly, the National Centers for Environmental Prediction) and has many model system components in common with its parent model, the Global Spectral Model (GSM). In the following experiments, dynamical downscaling of NCEP/National Center for Atmospheric Research (NCAR) Reanalysis (Kalnay et al. 1996) was performed. The model was run over three-month periods in summer (June–August 2000) and in winter (December 2000–February 2001) for several domain sizes at 60 km resolution.

2.1. Scale Selective Bias Correction Method

One of the components of the SSBC is to apply spectral damping to the tendency of variables. By applying implicit time scheme to ensure the numerical stability, the finite difference formulation is shown in Equation 1 as:

$$F_t^{new}(m,n) - F_{t-1}(m,n) = \left(F_t^{old}(m,n) - F_{t-1}(m,n)\right) - \alpha\left(F_t^{new}(m,n) - F_{t-1}(m,n)\right) \quad \text{(Eq. 1)}$$

F_t is a perturbation field spectral coefficient at wave numbers m and n (in the x and y directions, respectively) at time t in the spectral space. F_{t-1} is the spectral coefficient at one time step before. The superscripts "*old*" and "*new*" indicate the value before the damping and after the damping, respectively. α is the damping coefficient. Eq. (1) can be reformulated as:

$$F_t^{new}(m,n) - F_{t-1}(m,n) = \left(\frac{1}{1+\alpha}\right) \cdot \left(F_t^{old}(m,n) - F_{t-1}(m,n)\right) \quad \text{(Eq. 2)}$$

In principle, the damping scheme works to reduce the size of the original tendency by multiplying it by coefficient $1/(1+\alpha)$. We choose α=0.9 and apply the damping scheme every time step. The choice of α=0.9 indicates that the growth of selected long waves are reduced roughly to half. The results presented in this report are not sensitive to the choice of damping coefficient. This will be shown in Section 2.4.

The driving field of NCEP/NCAR Reanalysis is run on triangular 62-wave truncation (T62), with its Gaussian grid of roughly 200 km. It is safe to assume that large-scale features larger than 5–6 grids in size are well resolved in the global model. Therefore, the set of wavenumbers m and n are chosen such that the damping scheme is applied only to the long waves whose physical wavelengths are 1000 km or longer. Note that the use of physical wavelength implies different wavenumber nudging for different domain sizes. The damping is applied only to zonal and meridional wind components, uniformly on all sigma levels (UV damping) following

von Storch et al. (2000). The von Storch et al. (2000) research used varying nudging coefficients with height, but our results are found to be insensitive to vertical variations of coefficient. For the temperature (T) and humidity (Q), we simply set the area mean perturbations to zero (TQ correction), assuming that the UV damping is strong enough to reduce large-scale errors in the wave component of temperature and moisture. This assumption may need to be refined later, because the dominance of control (i.e., whether winds control mass, or mass controls winds) is dependent on the horizontal and vertical scale of the motion as well as on the latitude. In addition to the large-scale UV damping and TQ correction, the natural logarithm of surface pressure perturbation is set to the difference of that of the mean surface elevation between the regional fine-scale field and the base coarse field (surface pressure correction). This setting is meant to correct the anomalous pressure difference that builds up as the result of the surface elevation difference (derived from separate orography for global and regional) in the regional model and the global grid. All of these corrections together are referred to as the *Scale Selective Bias Correction* (SSBC) method hereafter. In some sections below, the root mean square difference (RMSD) of pressure height from the base field is used as a measure of regional model error. In these cases, RMSD is calculated for the field for which the scale smaller than 500 km is filtered out. This is done to assess the impact of the SSBC scheme in reducing the large-scale error in the regional domain by excluding the beneficial RMSD caused by the development of small-scale detail in the domain.

2.2. Reduction of Large-scale Errors

Figure 1a shows 500-hectopascal (hPa) height field difference between the control run (48x35 grids; 2880 km x 2100 km domain) of the regional model and the base reanalysis field, averaged over three months in the winter of 2000–2001. There is a positive bias that is as large as 10 m over the entire regional domain, with an increasing gradient towards the eastern one third of the domain. Such positive bias does not conform to the large-scale solution provided by the base field and could interfere with errors on smaller scales. Spectral tendency damping scheme (UV damping) suppresses the growth of waves that are approximately 1000 km or longer in wavelength. For this particular case, the large-scale biases are relatively simple in pattern in the east-west direction. The UV damping could not completely eliminate the wave two pattern, and the scheme worked more to reduce the area-wide positive bias. The RMSD of the large-scale pattern is reduced to within 6 m from the base field (Figure 1b). Figure 1c illustrates the spectrum of the field as a function of two-dimensional wave number. There is a slight reduction in the spectral coefficients of long waves.

In the same control experiment, the winter average 850-hPa height field shows a similarly large area-wide positive bias with a very large positive peak in the west (Figure 2a). The area-wide positive bias is eliminated in the SSBC run (Figure 2b), while the very large positive bias in the western half of the domain is reduced. In the spectrum (Figure 2c), the scales of the wave numbers 10 or larger seem to be modified along with large reductions in the amplitude of long waves, but the SSBC scheme does not modify the relative strength of spectral coefficients among different wave numbers. As a result, small-scale regional details that were not obvious under the large-scale positive bias become evident in the SSBC run. A few small-scale peaks that are as large as 10 m in difference from the base field exemplify this function of the scheme. In the same manner as the 500-hPa height field, large-scale biases are kept within 6 m or less in magnitude.

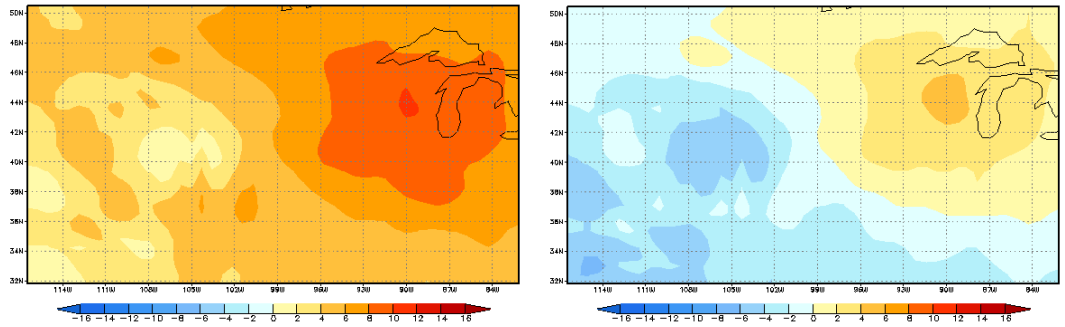

1a 1b

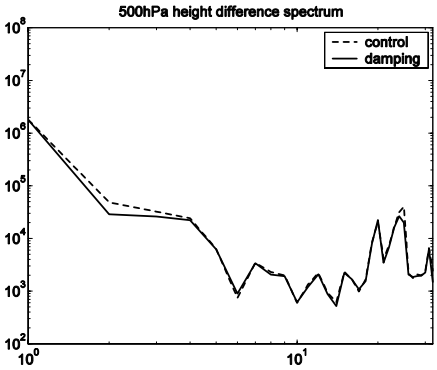

1c

Figure 1. 500-hPa height difference between the regional model and the reanalysis in the winter of 2000-2001. (a) control run, (b) SSBC run, and (c) spectrum of both runs.

As described in the previous section, the SSBC method consists of: (1) long wave tendency damping on winds (UV damping), (2) TQ correction, and (3) surface-pressure correction. It turns out that all these components are necessary to reduce large-scale biases effectively. In order to illustrate the complementary functions of correction components, further experiments were performed. Figure 3 shows the 500-hPa height difference between the regional model and the reanalysis field (base field) for the summer of 2000. Figure 3a is a control run without the full SSBC scheme. Figure 3b uses only the UV damping and TQ correction; Figure 3c shows the surface pressure correction run only; and Figure 3d is the simulation with all corrections. The UV damping and TQ correction (Figure 3b) are able to reduce the dominant negative peak in the middle of the domain, but most of the area shows negative bias. The surface pressure correction is able to push up the whole domain by a couple of meters, but the large negative peak is not reduced (Figure 3c). The scheme is only able to contain the large-scale errors within 6 m from the reanalysis field when all the corrections are combined.

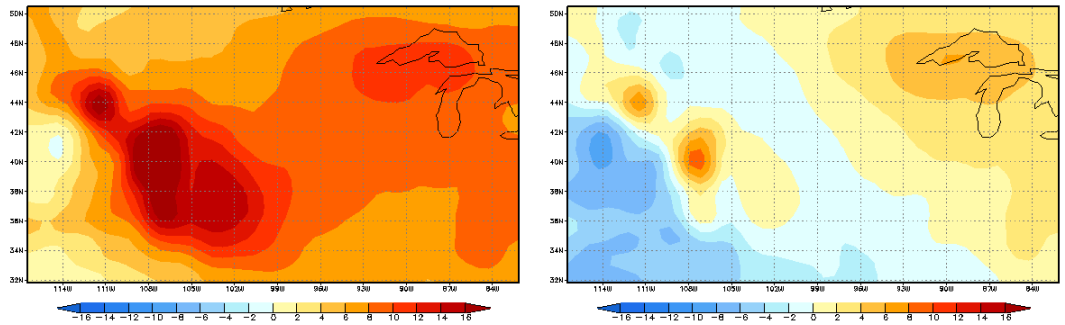

2a 2b

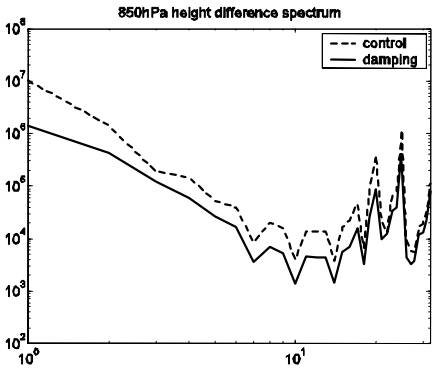

2c

Figure 2. Same as Figure 1 except for 850-hPa height.

In the large-scale damping part of the SSBC method, winds of the scale greater than 1000 km are damped, but temperature and humidity are corrected for the area-mean of perturbation only. As opposed to this, von Storch el al. (2000) applied spectral nudging scheme to the zonal and meridional wind components only. Their scheme adds nudging terms in the spectral domain in both directions, and they use a height-dependent nudging coefficient that is zero below 850-hPa and increases with height. The nudging coefficient is applied on the difference between the regional field and the base field (perturbation), as opposed to the SSBC scheme, which damps the tendency of the perturbation field. The RSM was run with von Storch's scheme to see how effective their scheme is compared to the SSBC. Table 1 shows the RMSD of 500-hPa height from the base field for different combinations of spectral nudging and SSBC components.

The no-SSBC case ends up with 11.2 m of RMSD and the spectral nudging reduces the error to 8.8 m. Our SSBC method can reduce the error to 3.9 m, so it is clear that the SSBC is more effective than spectral nudging alone. When only the part of SSBC that damps the longer wave of wind perturbation tendency (UV damping) is applied to the model, the simulation ends up with a comparable RMSD (8.5 m) to the spectral nudging alone.

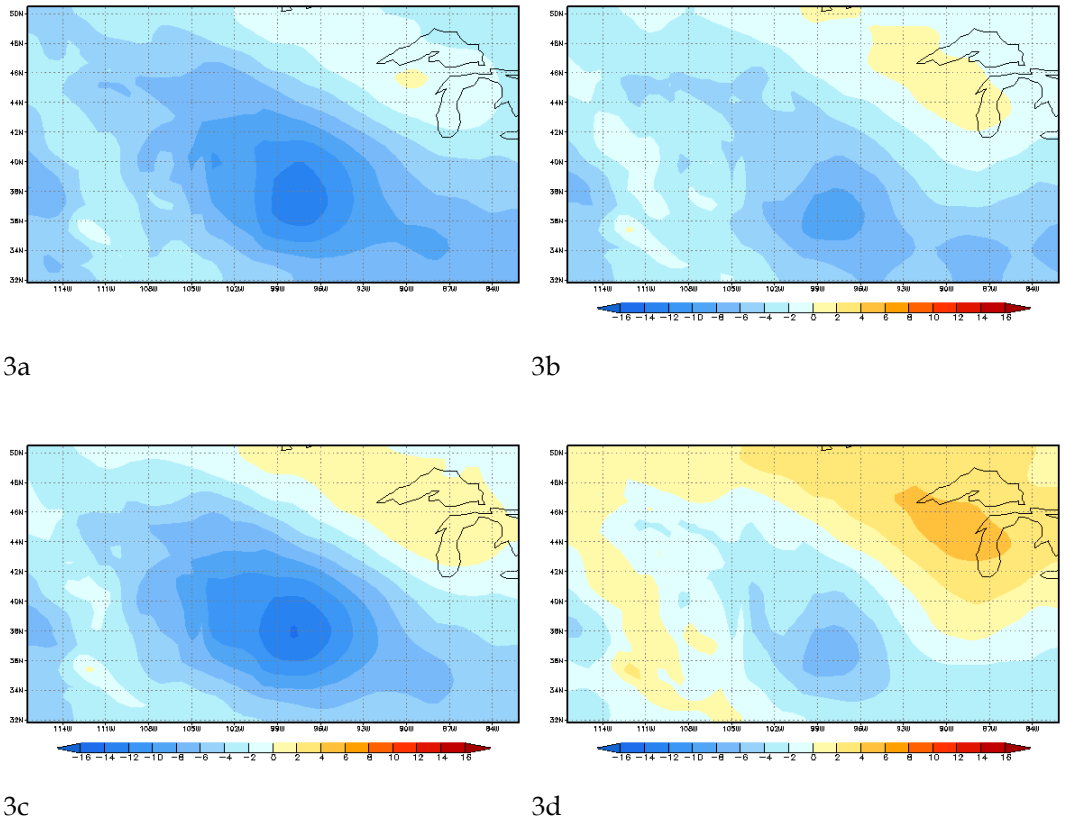

3a 3b

3c 3d

Figure 3. 500-hPa height difference between the regional model and the reanalysis in the summer of 2000. (a) control run, (b) long wave damping run, (c) surface pressure correction run, and (d) full SSBC run (both b and c).

Table 1. Root mean square difference of 500-hPa height from the base field in winter. RMSD is calculated at 500 km scale.

	No SSBC	Spectral nudging	UV damping	Spectral nudging + other SSBC functions	SSBC
RMSD (m)	11.2	8.8	8.5	4.0	3.9

In another run, the spectral nudging is complemented with two other components of SSBC (TQ correction and surface pressure correction). The package produces a similar RMSD (4.0 m) to SSBC. It appears that the spectral nudging and the UV damping have similar functions. For regional dynamical downscaling by RSM, TQ correction and surface pressure correction are important players in reducing large-scale errors. The relative importance of UV damping and TQ correction is discussed in Section 2.3.

2.3. Dependency of Dynamical Downscaling to Domain Size

Dynamically downscaled fields should be independent of the domain size, when forced by analysis. This discussion will demonstrate that the SSBC is a powerful method to make the downscaled analysis more independent of the selection of domain, compared to the conventional method. Let us suppose that we are interested in downscaling the domain size by half in both x and y directions (24x17 grids, 1440 km x 1020 km; domain B) from the domain in the previous experiment (48x35 grids, 2880 km x 2100 km; domain A). The third domain, C, is approximately 20% larger than domain A in both directions (60x43 grids, 3600 km x 2580 km) (Figure 4).

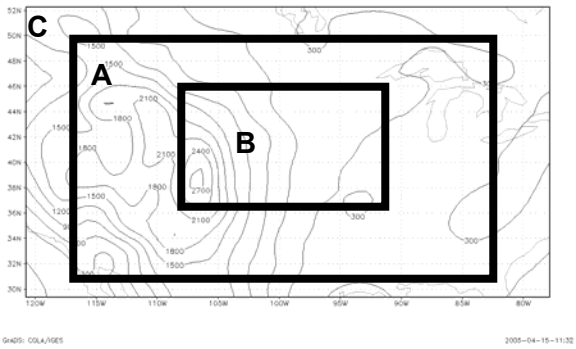

Figure 4. Three domain sizes for the experiment. (A) 48x35 grids, 2880 km x 2100 km; (B) 24x17 grids, 1440 km x 1020 km; and (C) 60x43 grids, 3600 km x 2580 km.

The three domains are centered in the same point but differ in the expansion. If the model generates very different solutions depending on the domain size, the use of dynamical regional downscaling is limited.

Figure 5 shows three panels of 500-hPa height deviation from the base field in the common domain (same as domain B) in the winter run. Domains A and C (Figure 5a and 5c) show similar positive large-scale patterns with 10 m maximum in the east, but they are clearly different from domain B, which is more positive over the entire domain on the order of 16 m or larger.

The SSBC method successfully eliminates the biases and the three domains produce strikingly similar patterns (Figure 6). The large-scale biases do not exceed 8 m with the scheme in any of the domain choices. RMSDs from the base field are calculated for each domain and experiment, as presented in Table 2. Although domain B has the largest errors in the control run, it is reduced by more than 80% in the SSBC run, and the errors in all three domains are less than 3 m.

Table 2. Root mean square differences of 500-hPa height difference between the regional model and the reanalysis field in winter of 2000-2001 calculated for the common area (domain B) at 500 km scale. The model was run on different domains expansion with the same center point.

	A	B	C
Control	5.9	15.1	7.6
SSBC	2.9	2.4	2.5

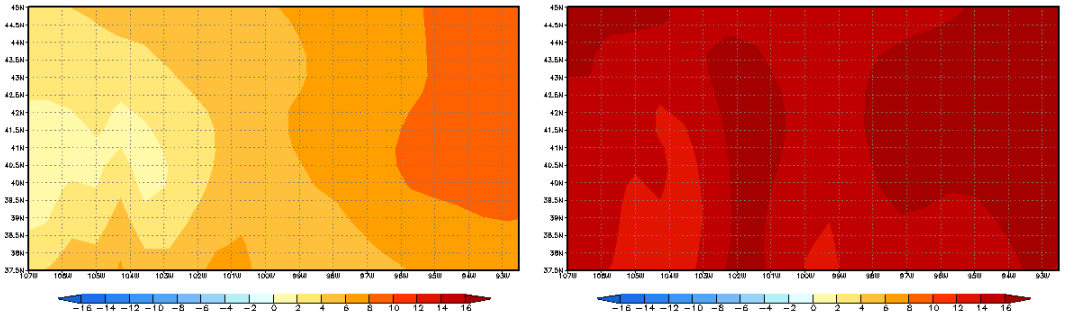

5a 5b

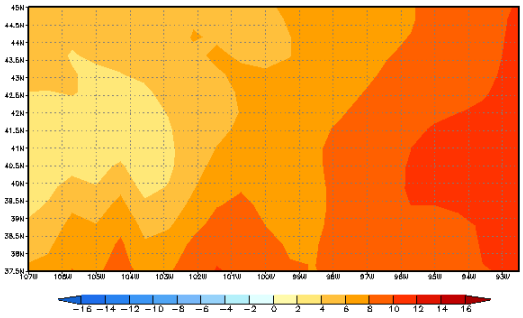

5c

Figure 5. 500-hPa height difference between the regional model and the reanalysis, run for different domain sizes and shown for the common area. The control run without SSBC scheme. (a) domain A (medium size), (b) domain B (half of domain A), and (c) domain C (20% larger than domain A).

As discussed in the previous section, UV damping, TQ correction, and surface pressure correction are complementary in the SSBC. In light of our interest in making consistent downscaling regardless of domain size, it is necessary to separate UV damping from TQ correction for discussion. In UV damping, u and v fields of the scale greater than 1000 km are damped, but in TQ correction, temperature and humidity are corrected for the area-mean perturbation only. This choice minimizes the use of the damping scheme, yet obtains the best performance from the scheme. For this experiment, the large domain is 96x69 grid points at 60 km covering the contiguous United States (5760 km x 4140 km), and the small domain is 24x17 grid points at the same resolution centered at 100°W and 41°N (1440 km x 1020 km). As for UV damping, only the wavenumber 1 is damped for the small domain, while wavenumbers 1 to 5 are damped in the large domain. TQ correction is in effect, regardless of the domain size. The difference in the effect of TQ correction and UV damping over domains with different sizes are highlighted. The experiments were conducted for the no-SSBC case, full SSBC case (with all three components), no-TQ correction, and no-UV damping case.

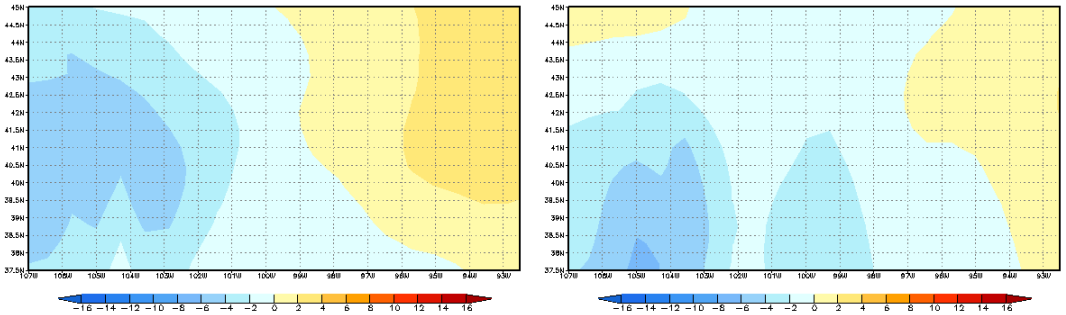

6a 6b

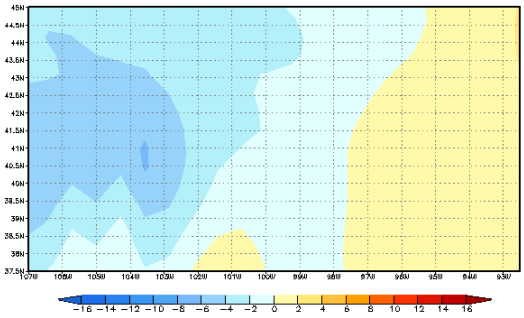

6c

Figure 6. Same as Figure 5, except for the SSBC run.

Figures 7 through 9 show the vertical profile of difference of area-mean specific humidity from the base field. In both small (Figure 7a) and large domains (Figure 7b), there is a large difference of area-mean humidity, up to 2×10^{-4} kilograms (kg)/kg. The no-SSBC run has the largest departure from the base field in the lower atmosphere. The full SSBC run reduces the area-mean humidity difference within 3×10^{-5} kg/kg in all levels. It turns out that this reduction comes largely from TQ correction. When the model is run without TQ correction, the simulation still results in large area-mean difference from the base field. The area-mean correction of humidity reduces the water content in the atmosphere at almost all levels. As a result, the wet bias in precipitation rate becomes smaller, as will be discussed in Section 2.6.

For the area-mean vertical profile of temperature, TQ correction plays a large part, as does the surface pressure correction (Figure 8a and b). In the no-SSBC case there are some pressure levels that have an excessively large magnitude of difference from the base field. The top layers of both small and large domain runs, for example, have more than 1 degree difference from the base field area-mean. Such large departures in temperature from the base field are suppressed within 0.2 degrees with the full SSBC run, but the no-TQ correction case still sees those large errors in the top layers. TQ correction is the only component of the scheme that is able to correct such errors. In other levels with moderately sized differences from the base field, both TQ correction and surface pressure correction are effective, because the three runs (full SSBC, no-TQ correction, and no SSBC) generate markedly different profiles. Large errors of

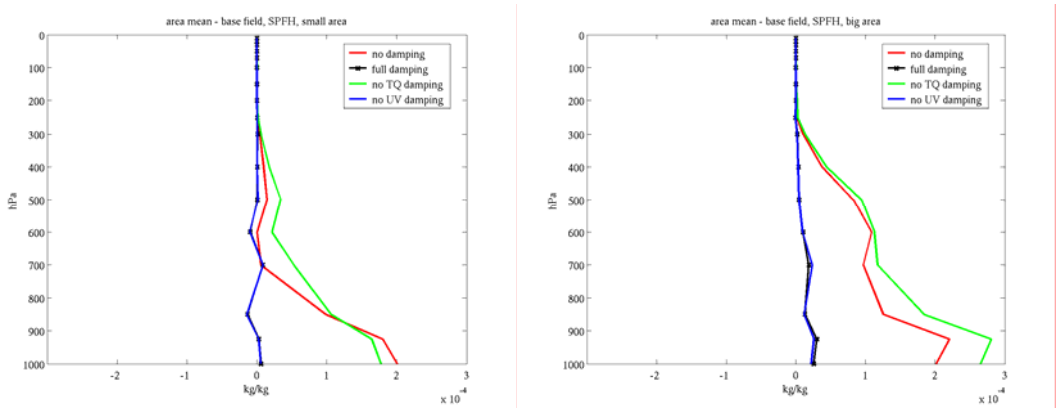

7a 7b

Figure 7. Area mean difference of specific humidity from the base field. (a) small domain, (b) large domain.

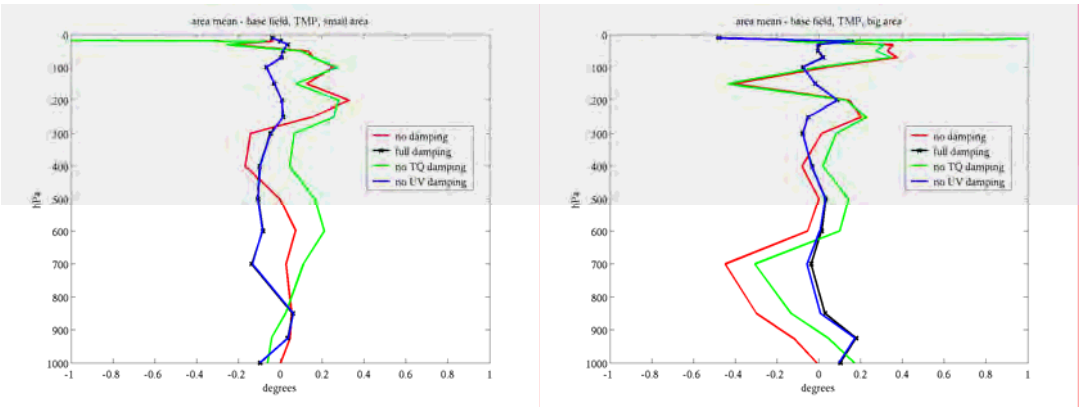

8a 8b

Figure 8. Area mean difference of temperature from the base field. (a) small domain, (b) large domain.

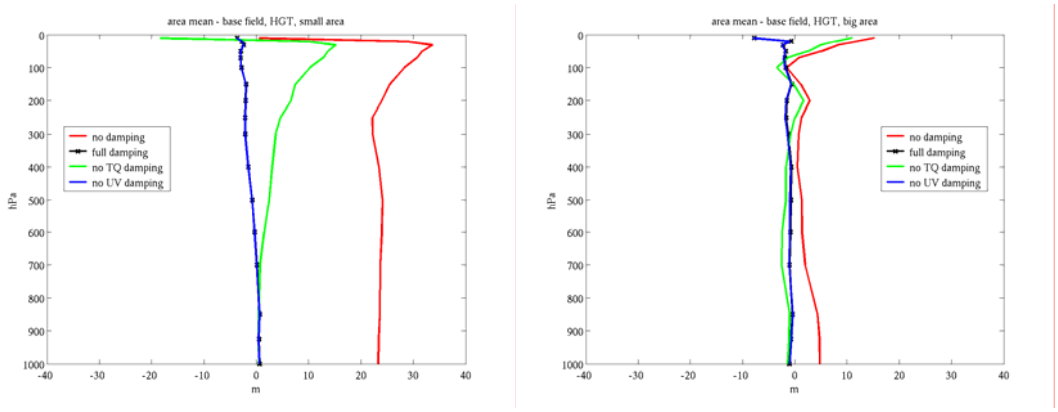

9a 9b

Figure 9. Area mean difference of pressure height from the base field. (a) small domain, (b) large domain.

temperature at the top layers are associated with pressure height errors at the same levels. Pressure height field is indirectly corrected by TQ correction as well as the surface pressure correction (Figure 9a and b). Both of these components are essential to the area-mean height difference profile in the vertical. TQ correction is, however, not a large part of SSBC in the lower atmosphere. One of the reasons why the spectral nudging of von Storch et al. (2000) does not work as well as the SSBC scheme in RSM is because the spectral nudging method changes only the large waves of winds, as discussed in Section 2.2. It is clear from these area-mean field analyses that TQ correction and surface pressure correction are necessary to nudge the large-scale state of regional downscaled field to the base field in RSM.

It appears that UV damping is not a large player when it comes to the vertical profile of area-mean variables, as indicated by similar profiles between the full SSBC run and the no-UV damping run. Nonetheless, the following experiments show that UV damping is essential in regional downscaling. Figures 10 and 11 show the difference of 500-hPa height from the base field. In the small domain, only the largest wave of u and v winds is damped, and its effect is minimal because the full SSBC case and no-UV damping case look alike (Figure 10a and b). The absence of UV damping is compensated by TQ correction. Comparison of the no-TQ correction case (Figure 10c) with the full SSBC case (Figure 10a) shows the effect of TQ correction on height field. Thus the UV damping is not effective in the small domain.

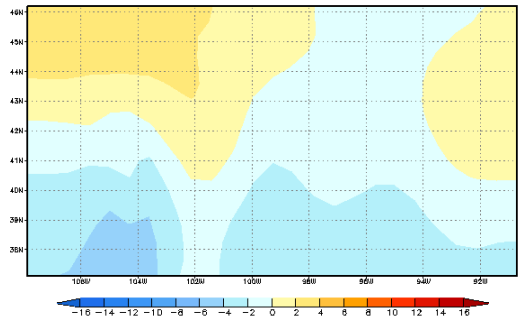

10a

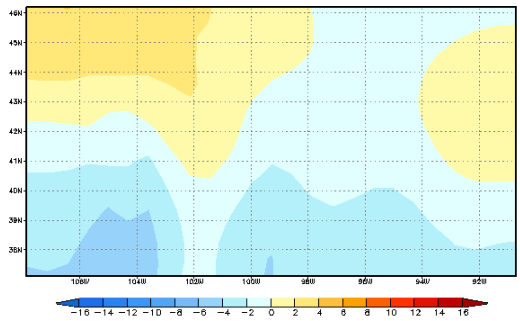

10b

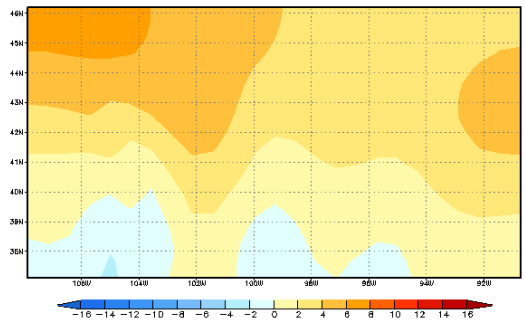

10c

Figure 10. 500-hPa height difference from the base field for the small domain. (a) full SSBC, (b) no-UV damping, (c) no-TQ correction.

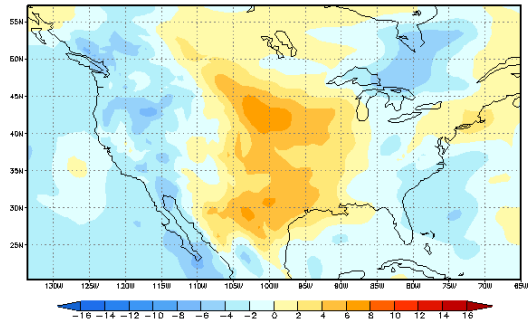

11a

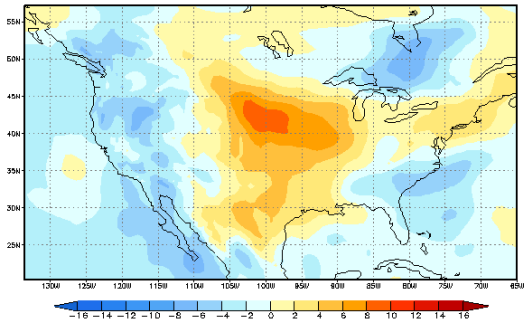

11b

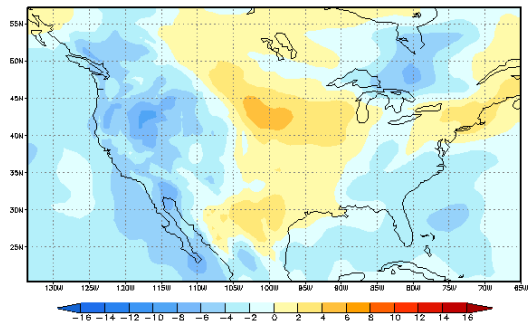

11c

Figure 11. 500-hPa height difference from the base field for the large domain. (a) full SSBC, (b) no-UV damping, (c) no-TQ correction.

In the large domain, the no-UV damping run turns off the damping of the first 1 to 5 wavenumbers of u and v. Its effect should be seen in the large-scale patterns that TQ correction cannot handle. The positive peak in the center of the domain and the two negative patterns in the east of the domain are larger in the no-UV damping case (Figure 11b) compared to the full SSBC case (Figure 11a). The RMSD is 2.8 m in the no-UV damping case, and 2.6 m in the full SSBC case. The UV damping reduces the amplitude of waves that those peaks represent in the spectral space, so both positive and negative patterns can be suppressed at the same time.

2.4. Dependency of Downscaling to Damping Coefficient

This section discusses tests that were conducted on the sensitivity of dynamically downscaled regional field to the choice of damping coefficient α. The experiments were conducted for α of 2, 5, 10, 20, and 100 in winter, and compared with the α=0.9 used in other control experiments. In the largest damping coefficient case, the tendency of the perturbation field for selected large waves of winds is reduced to roughly one-hundredth of the original, as opposed to one-half for the smallest coefficient. The RMSD of 500-hPa height is 6.0 m for January in the no-SSBC run. January simulations with varying damping coefficients result in a RMSD of 3.3 m or smaller, with a decreased RMSD for a larger damping coefficient up to 2.6 m for α =100 (Figure 12). But a 0.7 m reduction in the RMSD by using a large coefficient is not very significant, compared to the large RMSD in the no-SSBC case. The February no-SSBC case has a RMSD of 2.6 m, which is already a very small difference, so the SSBC scheme does not have much impact on the large-

scale field. The resulting RMSD for different damping coefficients are 2.5 to 2.9 m. It is not necessarily true that a larger damping coefficient leads to a smaller RMSD. In December, the RMSD is 12.6 m in the no-SSBC case, which is reduced to 2.5–2.7 m in the SSBC runs, but the largest damping coefficient (α =100) does not yield the smallest RMSD. It is possible for a different damping coefficient to make small differences in large-scale field but the difference in RMSD is always less than 1 m in 500-hPa height field. The choice of a larger damping coefficient is not justified by such a small difference. We chose to use the smallest coefficient as a default.

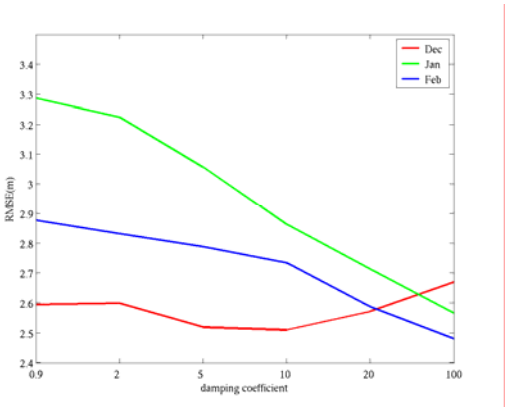

Figure 12. Root mean square difference of 500-hPa height from the base field for different damping coefficients.

2.5. Lateral Boundary Relaxation

In order to reduce the noise from the lateral boundaries, RSM uses a lateral boundary relaxation with implicit time scheme, which can be written as (Juang et al. 1997)

$$\frac{\partial A}{\partial t} = f - \mu\left(A^{t+1} - A_g{}^{t+1}\right) \qquad \text{(Eq. 3)}$$

where A is the full field obtained from regional integration, A_g is the full field value from the outer coarse grid, and f is the total forcing. μ is equal to $(1-\beta)/T$. T is the e-folding time. β is the coefficient and approaches zero along the lateral boundary zone, as shown in Section 3b of Juang and Kanamitsu (1994). The perturbation form of Eq. (3) can be rewritten as

$$\frac{\partial A'}{\partial t} = \frac{F - \frac{\partial A_g}{\partial t} - \mu A'^{n-1}}{1 + 2\mu\Delta t} \qquad \text{(Eq. 4)}$$

where Δt is the time step. Juang et al. (1997) found that this relaxation is very efficient with a larger e-folding time for any domain size even with mountains along the lateral boundaries.

One wonders about the relative importance of the relaxation and the SSBC in the regional dynamical downscaling. Both share the function of alleviating the inconsistencies between the

regional field and base field. The default e-folding time for the relaxation is 2400 seconds (sec), and the first experiment was done for varying e-folding time between 480 to 3600 sec without SSBC (Figure 13).

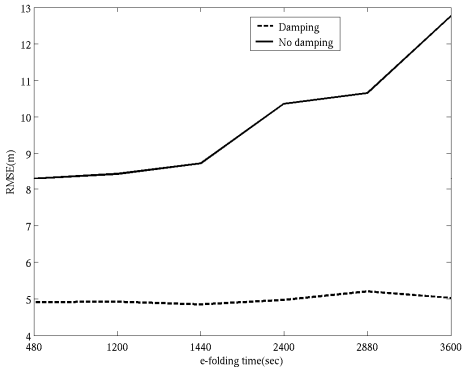

Figure 13. Root mean square difference of 500-hPa height from the base field for different boundary relaxation e-folding time.

The model simulation results in larger RMSD of 500-hPa height from the base field (reanalysis) when the relaxation is weaker (larger e-folding time). When the e-folding time is 480 sec, the RMSD is 8.3 m and RSME rose to 12.8 m when the e-folding time is 3600 sec. Although the relaxation has direct effects only near the boundary by design, it is applied in the grid space and its effect propagates in all spectrums of waves, so large-scale patterns are also affected by the strength of relaxation. The large anomaly in 500-hPa height difference from the base field is over 24 m when the relaxation is weak, but it is reduced to about 20 m when stronger relaxation is used. Without the help of spectral nudging, the easiest strategy to reduce the large-scale error is to decrease the e-folding time and apply a large boundary relaxation.

The second experiment uses both implicit boundary relaxation and SSBC. The RMSD is about 5 m, no matter how weak the boundary relaxation is. The SSBC is much more effective than the strongest boundary relaxation in reducing the 500-hPa height large-scale error. The downscaling runs with the SSBC are able to produce similar simulations, regardless of the strength of boundary relaxation. One is able to use a larger e-folding time and reduce the impact of relaxation, when the relaxation is used with the SSBC. It is not possible, however, to run the model without the relaxation. Our experiments show that the model immediately becomes unstable without the relaxation when the SSBC is turned on. The boundary relaxation is necessary to stabilize the small-scale unstable wave excited by the lateral boundary because the SSBC is only applied to large waves and area means. The relaxation is still an essential part of the numerical model even when used together with the SSBC.

2.6. Comparison with Observation

Large-scale errors in the regional domain could interfere with small-scale dynamics and distort variability in fields such as precipitation. This section assesses the performance of the model when SSBC scheme is applied. For the assessment, the model is run for a very large domain that covers the entire continental United States (96x69 grids), with and without the SSBC scheme. Such a very large model domain ensures a fair skill test of precipitation field against observation. The precipitation observation used for verification is Higgins' gridded daily precipitation for the

United States (Higgins et al. 1996). Table 3 shows the equitable threat score and bias score for the RSM runs in winter and summer. The bias score measures the relative area of simulated and observed precipitation. A perfect score (1) indicates the simulated precipitation area is the same as observed. Bias larger than 1 means overestimated rainfall and bias smaller than 1 means underestimated rainfall. The equitable threat score is the ratio of the correct simulated area to the total area of the simulated and observed precipitation. The score gets penalized for simulating rain in the wrong place as well as not simulating rain in the right place. The higher the value, the better the model skill is for the particular threshold. The scores are computed for the grids that have precipitation above 0.2 millimeters (mm) day^{-1}.

Table 3. Precipitation threat scores and bias scores.

	Summer		Winter	
	Threat	Bias	Threat	Bias
Control	0.40	0.95	0.44	1.47
SSBC	0.42	0.97	0.46	1.14

In both seasons threat scores are increased and bias scores are brought closer to 1 in the SSBC runs. In summer, on 60 days out of 92 days threat scores improved by as much as 0.2. Biases are corrected on 55 days. Similarly in winter, threat scores improved on 62 days and bias scores on 71 days out of 90 days. The SSBC demonstrates similarly good skills regardless of season. In other precipitation thresholds of control run ranging from 0.01 to 1.00 mm day^{-1}, summer has dry biases in smaller precipitation range and wet biases in large precipitation, while winter shows wet biases, regardless of precipitation amount. Both threat scores and bias scores are improved by the SSBC scheme in all precipitation thresholds.

Figure 14 shows precipitation fields above 0.2 mm day^{-1} on June 26, 2000. For this day, the threat score improved from 0.42 to 0.53 and the bias score from 0.75 to 0.92 in the SSBC run. The control run (Figure 14a) has less area of precipitation than the observation (Figure 14c). In the control run, precipitation appears in the southern Great Lakes region, but actual measurements indicate that it did not rain in that area. The observation shows precipitation in the Northeast, and over Louisiana and eastern Texas, as well as directly to the west of the Great Lakes. Those precipitations are absent in the control run. In the SSBC run (Figure 14b) these deficiencies in the control run have been corrected. The area of precipitation in the southern Great Lakes region breaks up and one part shifts to the west of the Great Lakes while the other moves to the Northeast, although it does not extend as far northeast as the observation. There is more precipitation over Louisiana as well. The change in the precipitation pattern roughly corresponds to that of the precipitable water pattern. Figure 14d shows the difference in precipitable water filed between the SSBC run and the control run. Where there is less precipitable water (south of the Great Lakes), less precipitation is simulated in the SSBC run. There are two bands of increased precipitable water located directly north and south of the decreased precipitable water band, and they correspond to the area of increased precipitation in

the SSBC run. Over Louisiana, precipitable water is slightly increased when the precipitation amount is increased as well.

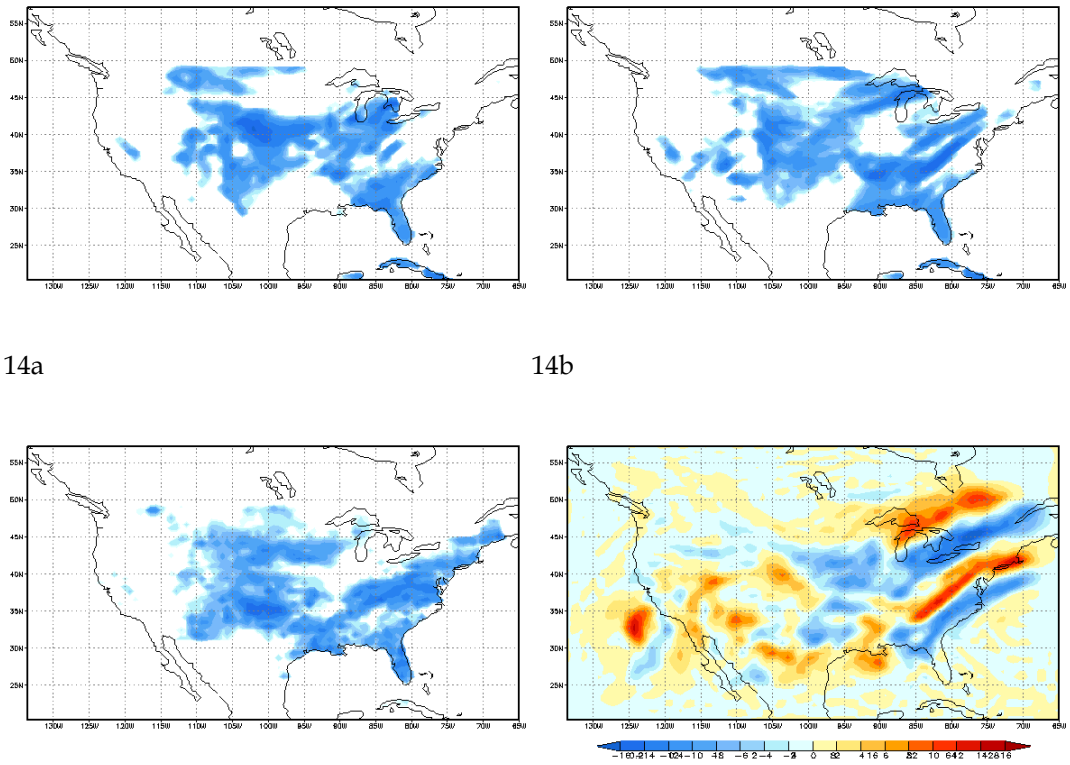

14a 14b

14c 14d

Figure 14. June 26, 2000 precipitation field above 0.2 mm day^{-1}. (a) control run, (b) SSBC run, (c) observation, and (d) precipitable water difference between the SSBC run and the control run.

Another example of improved precipitation fields is a correction of wet bias on February 14, 2001. The control run (Figure 15a) shows far too much precipitation in the central United States, compared to the observation (Figure 15c). The precipitable water difference field between the SSBC run (Figure 15d) and the control run indicates that the control run overestimated precipitable water for most of the country. The SSBC run eliminated this large bias, which led to a marked absence of precipitation in the middle of the continent. A significant decrease of precipitable water from eastern Texas to Florida corresponds to the southern portion of the decreased precipitation area in the SSBC run. The threat score increases from 0.38 to 0.51 and the bias score is reduced from 1.75 to 0.91. In both cases, the correction of large-scale dynamics errors positively influenced the small-scale variability of such fields as precipitable water, and the precipitation field compares better against observation.

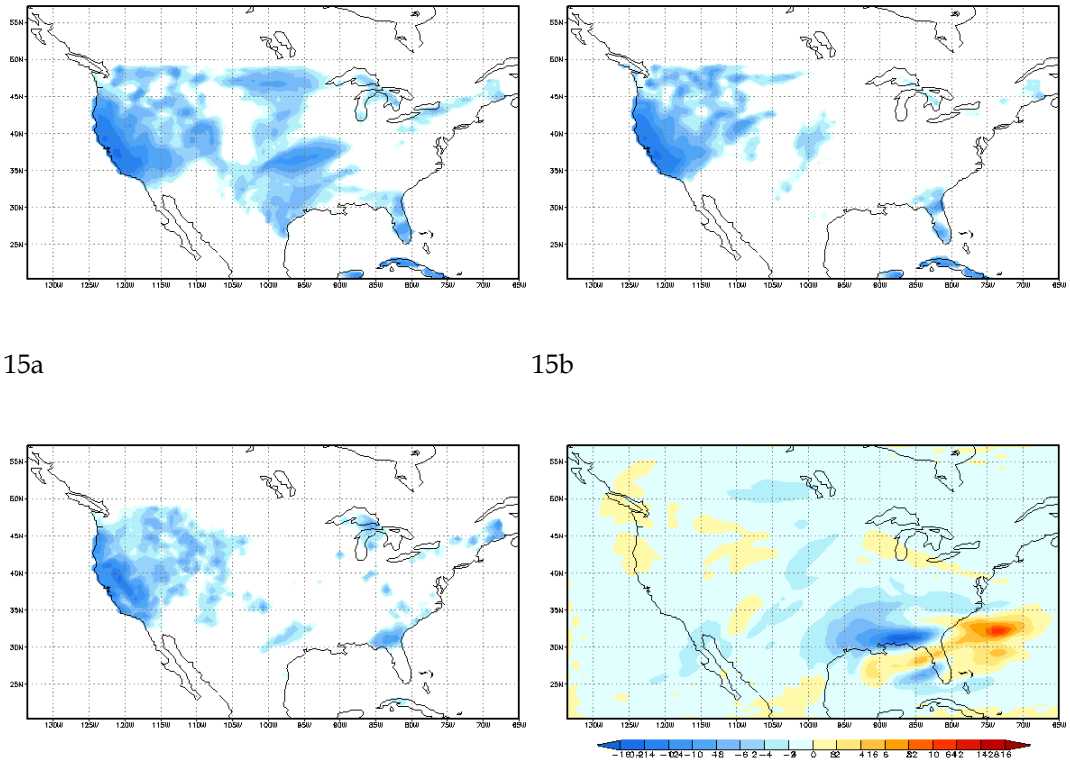

15a 15b

15c 15d

Figure 15. February 14, 2001 precipitation field above 0.2 mm day^{-1}. (a) control run, (b) SSBC run, (c) observation, and (d) precipitable water difference between the SSBC run and the control run.

2.7. Climatology of Surface Fluxes with SSBC

This section looks at the climatology of surface fluxes and compares the SSBC run to the run without the scheme. For validation purposes, reanalysis fields are presented with the exception of precipitation, which was discussed in detail in the previous section using observations. Downscaled analysis and reanalysis have comparable magnitude, but there are apparent regional differences in many variables, and those differences are discussed here. Figures are presented by subtracting the area-mean of the variable to focus on the spatial distribution, rather than the magnitude. In most cases the SSBC run and the control run (no SSBC run) look similar, so the difference between the two is also presented. Figure 16a shows total cloud cover for the summer of 2000 in the control run, and Figure 16b is for the SSBC run. There is less cloud cover in the middle of the continent, and near the coast in the West. More cloud cover is seen in the Northeast and the mountain areas in the West. This is where a marked difference from the coarse resolution reanalysis is seen (Figure 16d). Figure 16c shows the difference between the SSBC run and the control run. In the SSBC run, compared to the control run, there is less cloud cover in Arizona, New Mexico to Mexico in the south, Oregon, Nevada and much of the Northwestern region, and around the Great Lakes.

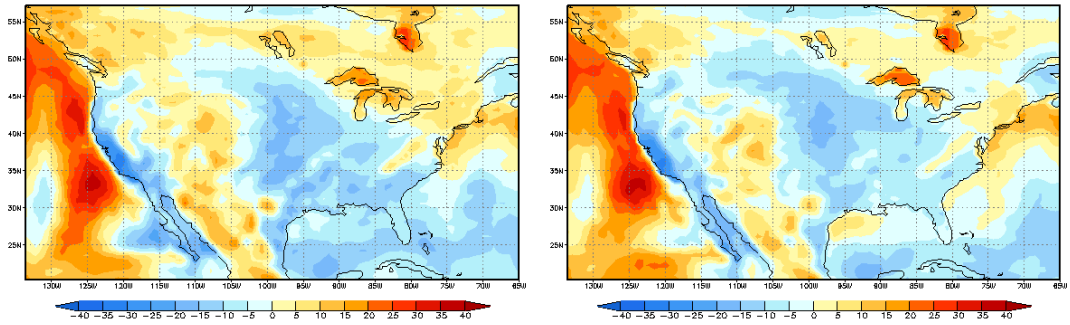

16a 16b

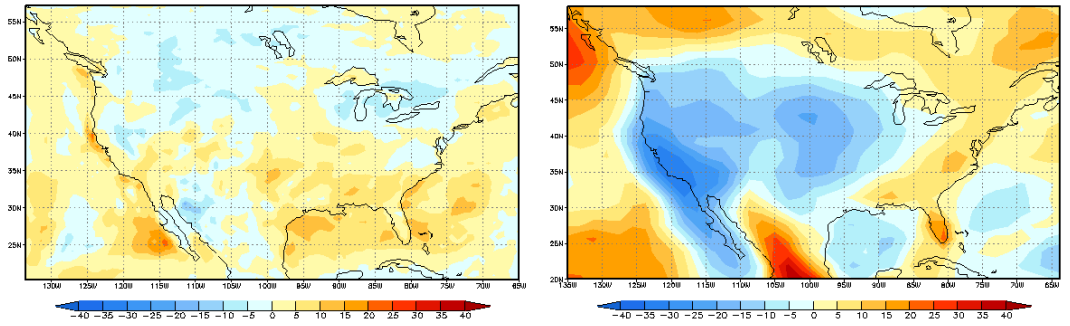

16c 16d

Figure 16. Total cloud cover field (%, area-mean subtracted) in summer. (a) no SSBC, (b) SSBC, (c) SSBC – no SSBC, (d) reanalysis.

These regions correspond to the areas with larger downward solar radiation at the surface (Figure 17c). In fact, most parts of the United States receive more solar radiation in the SSBC run, but the most pronounced increases are due to the cloud cover change. The downward solar radiation spatial pattern is similar to reanalysis but with many regional details (Figure 17d).

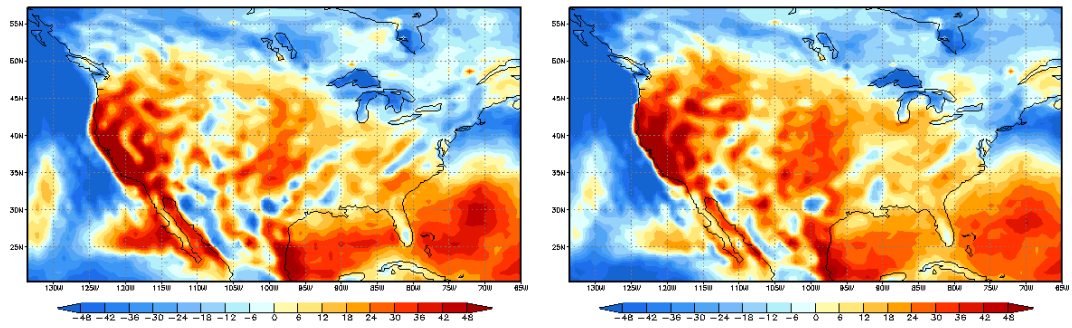

17a 17b

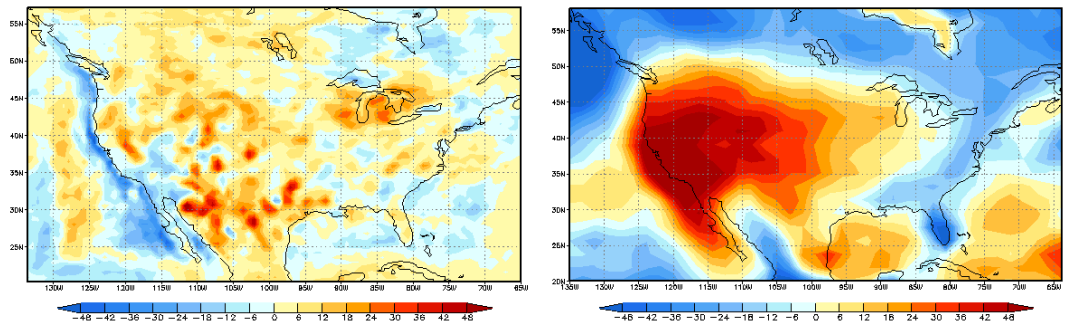

17c 17d

Figure 17. Downward solar radiation at the surface (W/m^2, area-mean subtracted) in summer. (a) no SSBC, (b) SSBC, (c) SSBC – no SSBC, (d) reanalysis.

The latent heat flux is large in the Rockies and along the Southeastern coast (Figure 18a and b). The area from the Great Lakes to the Northeastern coast—as well as that of Arizona, Utah, and Nevada—has less evaporation. These areas are noticeably different from the reanalysis (Figure 18d). The change by the SSBC scheme is small (within 20 watts per square meter (Wm^{-2})) with a few scattered localized large changes centered in the west (Figure 18c). These local increases in latent heat fluxes are compensated by the decrease in outgoing longwave radiation (OLR) to maintain the energy balance at the surface (Figure 19c). Other than the scattered hot spots in the west, the surface is generally warmer in the interior of the continent and colder in the Northeast and along the Eastern and Southern coastlines. The spatial pattern of OLR shows a good agreement with reanalysis (Figure 19 a, b, and d).

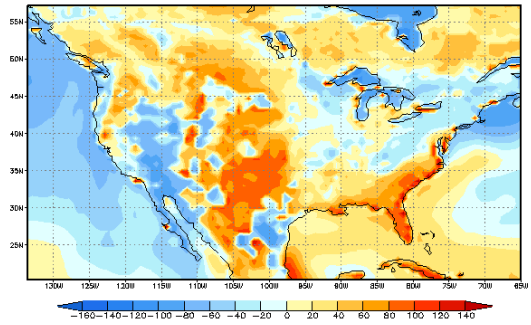

18a

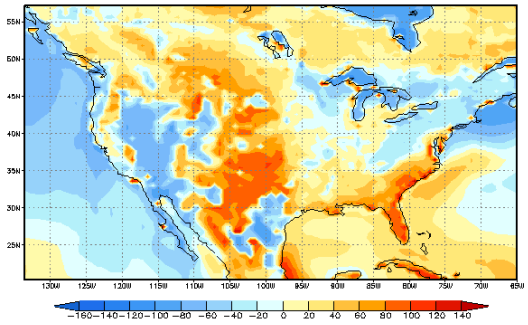

18b

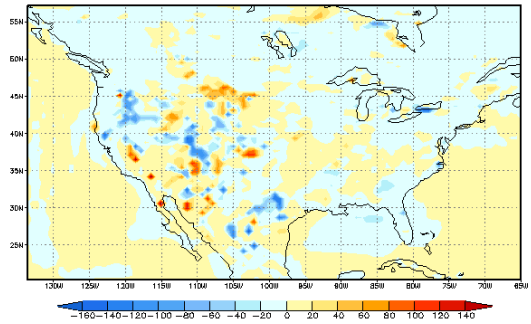

18c

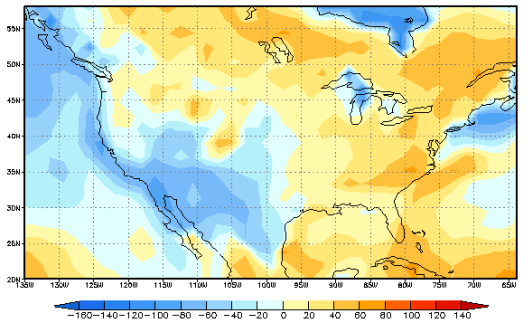

18d

Figure 18. Latent heat flux at the surface (W/m^2, area-mean subtracted) in summer. (a) no SSBC, (b) SSBC, (c) SSBC – no SSBC, (d) reanalysis.

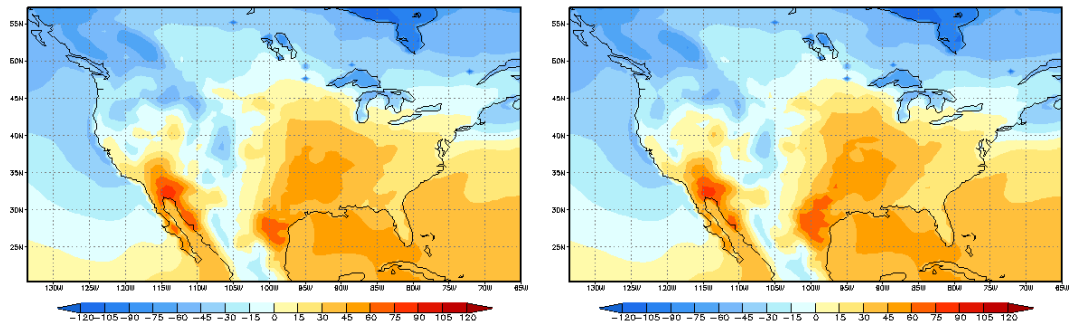

19a 19b

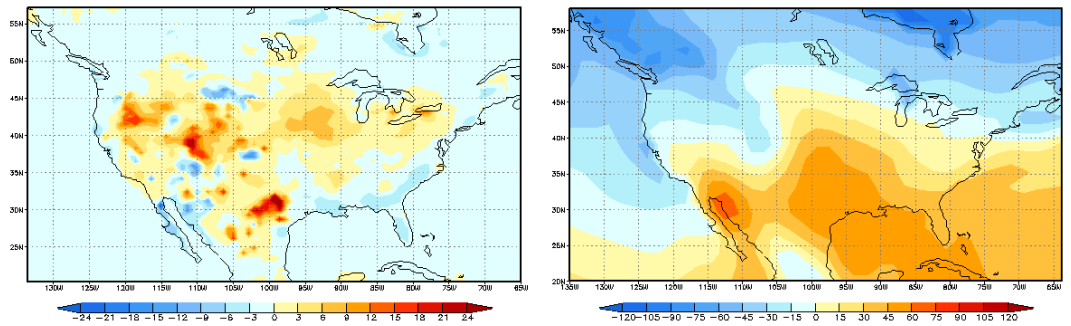

19c 19d

Figure 19. Outgoing long wave radiation at the surface (W/m^2, area-mean subtracted) in summer. (a) no SSBC, (b) SSBC, (c) SSBC – no SSBC, (d) reanalysis.

The dominant change in the precipitation field after SSBC is a decrease of precipitation over land, but there are also many areas of increased precipitation scattered throughout the country (Figure 20c). There is no systematic shift in the precipitation field but the change is localized with a general decrease of overall precipitation. Areas with increased (or decreased) evaporation (Figure 20c) receive more (or less) precipitation, but the precipitation increase is not limited to the areas with evaporation change (Figure 20c).

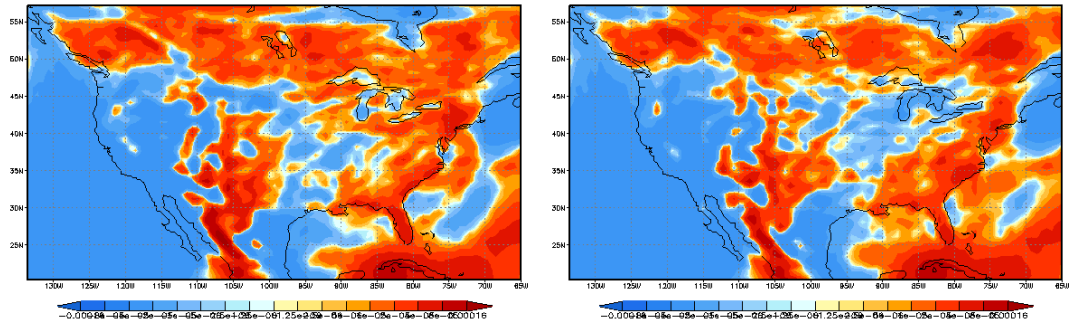

20a 20b

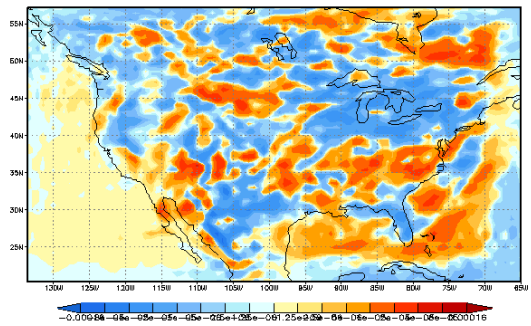

20c

Figure 20. Precipitation rate (kg/m^2/s, area-mean subtracted) in summer. (a) no SSBC, (b) SSBC, (c) SSBC – no SSBC.

Spatial patterns of these surface fluxes generally showed a good fit between the regional model and reanalysis in summer, but not in winter. Figure 21 shows the total cloud cover in winter. Cloudy areas are over the Great Lakes and the Northwest, but the positive pattern in the Northwest does not correspond to the reanalysis (Figure 21d). A positive field of solar radiation, for example, is centered farther south from the reanalysis (Figure 22 a, b, and d). Evaporation is very large over the Caribbean and off the East Coast, in contrast with reanalysis, that shows the lowest flux in the West (Figure 23 a, b, and d). The OLR shows a similar north-south pattern in both downscaled field and reanalysis, but the gradient is much higher in the regional model than reanalysis (Figure 24 a, b, and d).

The change in surface fluxes by the SSBC scheme in winter is simpler than in summer. The SSBC run produces less cloud cover over most of the continent (Figure 21c). As a result, the downward solar radiation at the surface increases all over the country (Figure 22c). There are no areas with a large latent heat flux change as in summer (Figure 23c). The outgoing longwave radiation decreases over most of the continent. The decrease is particularly pronounced to the west of the Great Lakes (Figure 24c). Precipitation decreases over most of the country, with a few increased spots in the middle of the country, and in the South (Alabama, Georgia, and South Carolina) (Figure 25c). As discussed in the previous section, a wet bias is corrected in the SSBC run.

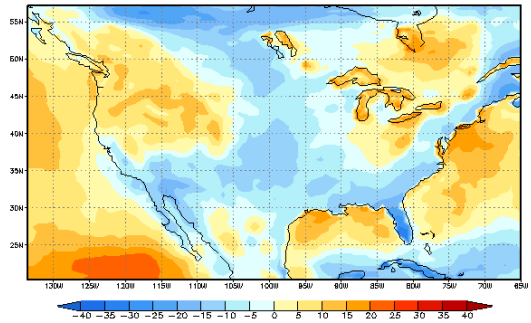

21a

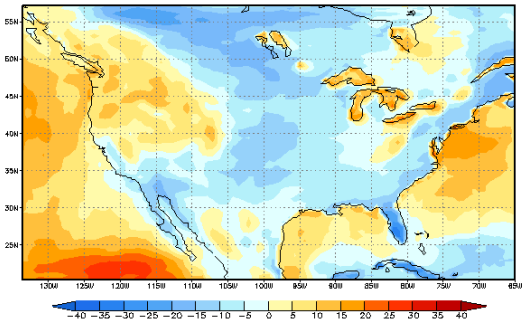

21b

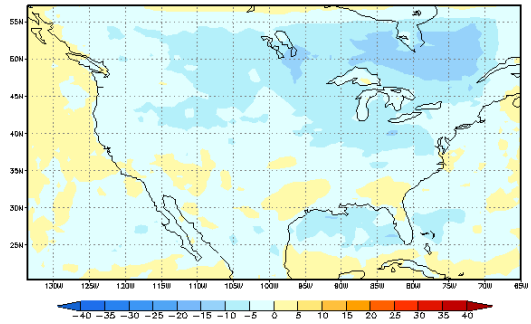

21c

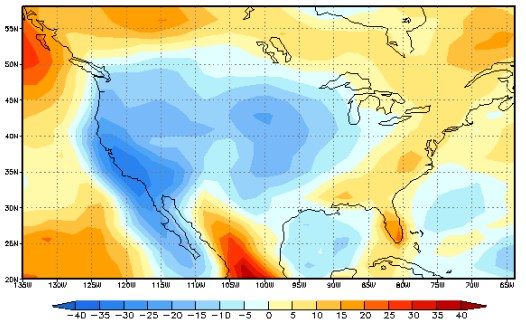

21d

Figure 21. Total cloud cover field (%, area-mean subtracted) in winter. (a) no SSBC, (b) SSBC, (c) SSBC – no SSBC, (d) reanalysis.

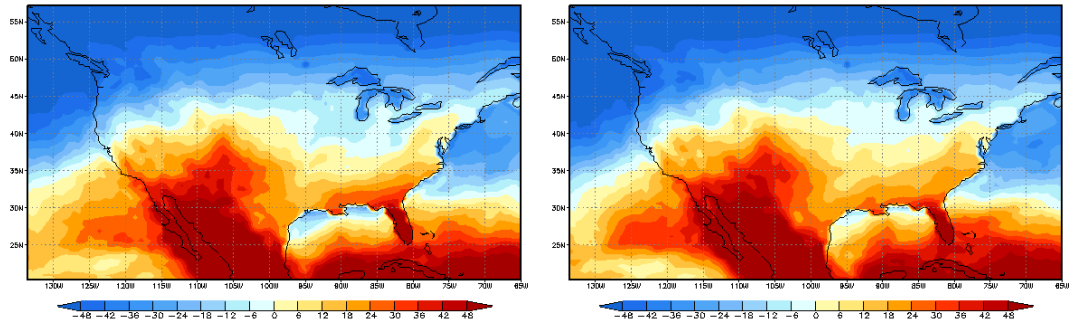

22a 22b

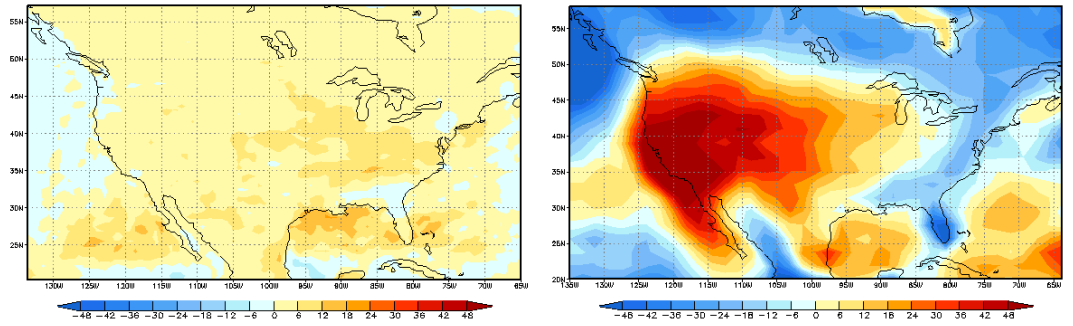

22c 22d

Figure 22. Downward solar radiation at the surface (W/m^2, area-mean subtracted) in winter. (a) no SSBC, (b) SSBC, (c) SSBC – no SSBC, (d) reanalysis.

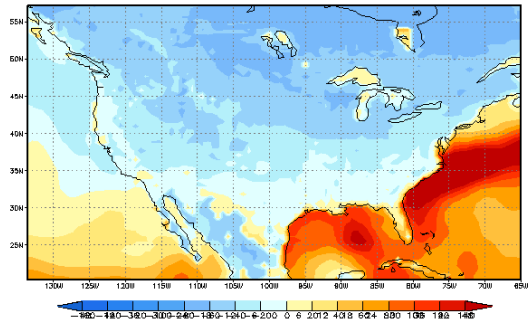

23a

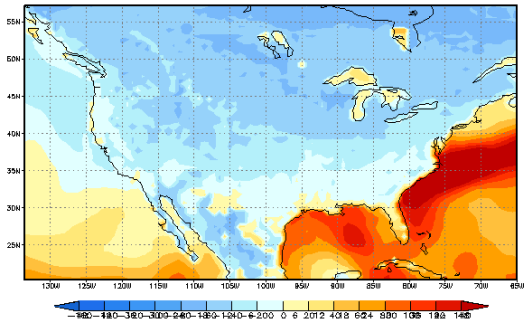

23b

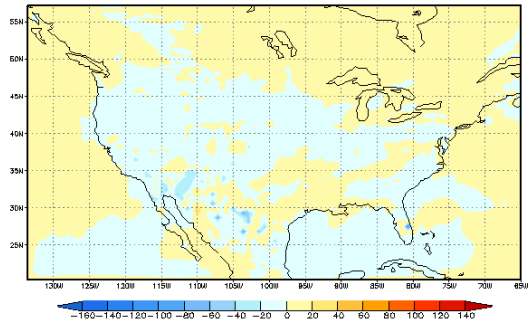

23c

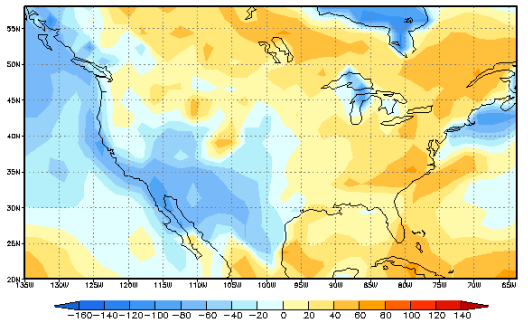

23d

Figure 23. Latent heat flux at the surface (W/m^2, area-mean subtracted) in winter. (a) no SSBC, (b) SSBC, (c) SSBC – no SSBC, (d) reanalysis.

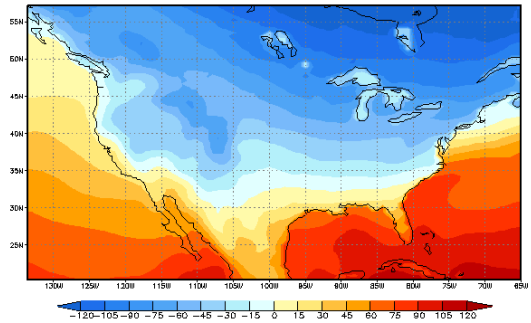

24a

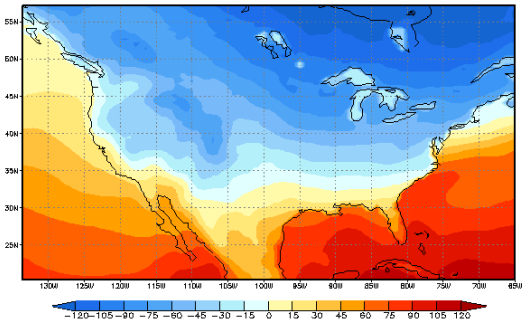

24b

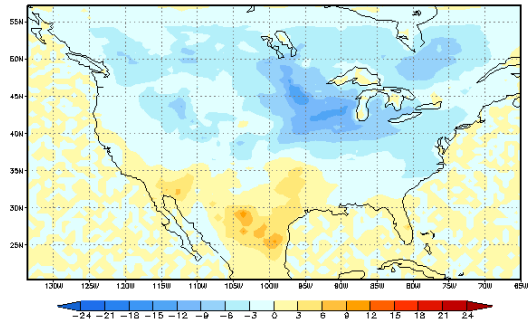

24c

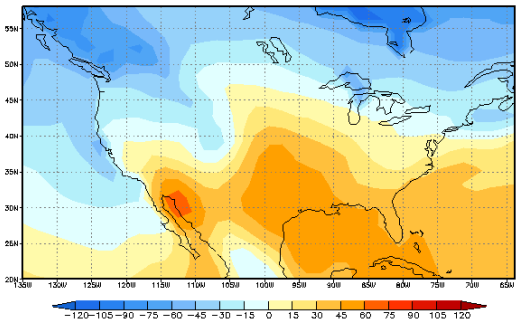

Figure 24. Outgoing long wave radiation at the surface (W/m^2, area-mean subtracted) in winter. (a) no SSBC, (b) SSBC, (c) SSBC – no SSBC, (d) reanalysis.

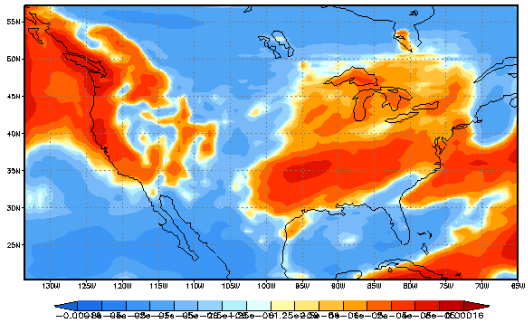

25a

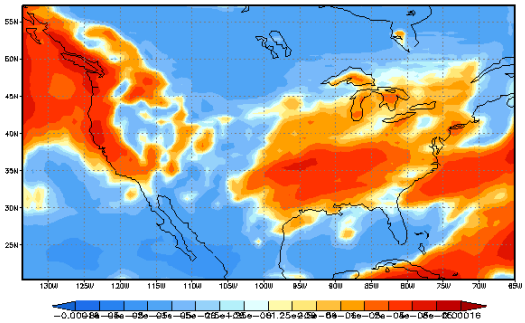

25b

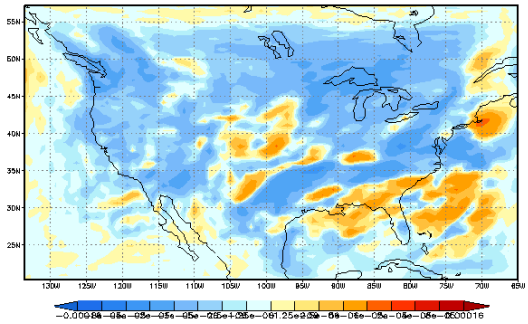

25c

Figure 25. Precipitation rate (kg/m^2/s, area-mean subtracted) in winter. (a) no SSBC, (b) SSBC, (c) SSBC – no SSBC.

Because large-scale differences in the atmospheric variables are minimized by the use of the SSBC scheme, the large-scale differences in the fields between simulation and Reanalysis are considered to be caused mainly by the difference in model physics between the RSM and the Reanalysis, namely the convective parameterization and radiation. In general, large scale components of the fields are very similar between the uncorrected and corrected runs in terms of deviation from the domain average, but a significant difference is found in small scale detail, indicating the significant impact of the SSBC procedure to the small scale that is not affected by the scheme.

3.0 Conclusions

Like any other regional climate model, the Regional Spectral Model is not free from the growing large-scale errors in the regional domain. Despite the use of the global model field not only in the lateral boundary, but also in the inner domain for defining perturbation in the RSM, the model has no explicit forcing towards global model field in the interior of the regional domain. A correction method to reduce large-scale errors in the RSM dynamical downscaling was formulated. One component of the method is to damp the tendency of selected long wave spectral coefficients of zonal and meridional components of wind, at every time step. The cutoff scale of 1000 km was used as the smallest scale the global reanalysis provides as reasonably accurate. In addition, domain-averaged temperature and humidity perturbations are set to zero. The surface pressure difference between the model field and the global field is also corrected. These corrections are collectively named the *Scale Selective Bias Correction* (SSBC) scheme.

The SSBC scheme is applied to the downscaling experiments of NCEP/NCAR Reanalysis. The scheme successfully removes large-scale errors in the dynamics field from 500-hPa height both in summer and winter. The departure of 500-hPa height from the reanalysis field of scale greater than 500 km does not generally exceed 8 m.

Conventional regional climate models could produce an undesirably different picture of downscaled fields, depending on the choice of domain size. This shortcoming has largely proved to be due to the large-scale errors that can be reduced by the SSBC scheme. It was demonstrated that the three components of the SSBC scheme are best used together as a package. TQ correction and surface pressure correction are effective no matter how large the domain size. UV damping becomes more important for a larger domain. UV damping is similar in function to the spectral nudging of von Storch et al. (2000), but for RSM the other two functions of SSBC are indispensable.

The optimal coefficient for damping is hard to select without a good measure to determine the skill of the model. Varying coefficients resulted in relatively small differences in 500-hPa height RMSD, so the smallest coefficient was chosen as default. Lateral boundary relaxation is still a necessary technique for stable model integration, even with SSBC. With the use of the SSBC scheme, one can use a larger e-folding time for boundary relaxation because it reduces large-scale errors more effectively than relaxation.

This project demonstrated that the SSBC scheme improves the simulation of such fields as precipitation because small-scale dynamics are no longer disrupted by large scale errors. Experiments are performed over the entire continental United States and precipitation threat scores increase by about 0.02 in both seasons. The wet bias in winter and dry bias in summer are significantly corrected. Such improvements in the precipitation field resemble patterns of precipitable water change, which responds to the change in the large-scale field. It is not easy to assess the direct benefit of the SSBC scheme on a smaller domain in which precipitation scores are not accurately estimated, but the continental domain experiments proved the scheme's ability to improve the regional scale fields.

The change in surface fluxes by SSBC is described in the last section. Summer and winter are effected very differently. Summer has more localized changes as opposed to winter, which has relatively uniform changes over land. The SSBC has an impact not only on large scale, but also

on the small scales forced by the background field through changes in large-scale circulations, moisture availability, and static stability.

The bias correction method proposed in the paper is not designed only for the Regional Spectral Model. The method is relatively easily applied to conventional grid point regional models, by calculating the difference from the background field over the domain, and applying sine and cosine transforms. It is recommended that when regional models are used for climate simulations such as dynamical downscaling of reanalysis, one must ensure that the large-scale errors are corrected by some method, which would lead to better skill, and consistent downscaled products that are independent of the choice of domain.

REFERENCES

Davies, H. C., 1976: A lateral boundary formulation for multi-level prediction models. *Quart. J. Roy. Meteor. Soc.*, **102,** 405-418.

Higgins, R. W., J. E. Janowiak, and Y.-P. Yao, 1996: A gridded hourly precipitation data base for the United States (1963-1993). NCEP/Climate Prediction Center Atlas 1, National Centers for Environmental Prediction, 46pp.

Hoyer, J. M., 1987: The ECMWF spectral limited area model. *ECMWF Workshop Proc. On Techniques for Horizontal Discretization in Numerical Weather Prediction Models,* 343-359.

Juang, H.-M. H., and M. Kanamitsu, 1994: The NMC Nested Regional Spectral Model, *Mon. Wea. Rev.*, **122**, 3-26.

Juang, H.-M. H., S.-Y. Hong, and M. Kanamitsu, 1997: The NCEP Regional Spectral Model: An Update, *Bull. of Amer. Meteor. Soc.*, **78(10)**, 2125-2143.

Kalnay, E. and Co-authors, 1996: The NCEP/NCAR 40-Year Reanalysis Project. *Bull. of Amer. Meteor. Soc.*, **77**, 437-471.

Miguez-Macho, G., G. L. Stenchikov, and A. Robock, 2004: Spectral nudging to eliminate the effects of domain position and geometry in regional climate model simulations, *J. of Geophys. Res.*, **109**, D13104, doi:10.1029/2003JD004495.

von Storch, H., H. Langenberg, and F. Feser, 2000: A spectral nudging technique for dynamical downscaling purposes, *Mon. Wea. Rev.*, **128**, 3664-3673.

Waldron, K. M., J. Paegle, and J. D. Horel, 1996: Sensitivity of a spectrally filtered and nudged limited-area model to outer model options, *Mon. Wea. Rev.*, **124**, 529-547.